

# VLBI Observations of Water Masers in Onsala 1: Massive Binary Star Forming Site?

Takumi NAGAYAMA,<sup>1</sup> Akiharu NAKAGAWA,<sup>2</sup> Hiroshi IMAI,<sup>2</sup> Toshihiro OMODAKA,<sup>2</sup>  
and Yoshiaki SOFUE<sup>2</sup>

<sup>1</sup>*Graduate School of Science and Engineering, Kagoshima University,  
1-21-35 Kôrimoto, Kagoshima 890-0065*

<sup>2</sup>*Faculty of Science, Kagoshima University, 1-21-35 Kôrimoto, Kagoshima 890-0065  
nagayama@astro.sci.kagoshima-u.ac.jp*

(Received 2007 September 4; accepted 2007 November 8)

## Abstract

We present proper motions of water masers toward the Onsala 1 star forming region, observed with the Japanese VLBI network at three epochs spanning 290 days. We found that there are two water maser clusters (WMC1 and WMC2) separated from each other by  $1''.6$  (2900 AU at a distance of 1.8 kpc). The proper motion measurement reveals that WMC1 is associated with a bipolar outflow elongated in the east-west direction with an expansion velocity of  $69 \pm 11$  km s<sup>-1</sup>. WMC1 and WMC2 are associated with two 345 GHz continuum dust emission sources, and located  $2''$  (3600 AU) east from the core of an ultracompact H II region traced by 8.4 GHz radio continuum emission. This indicates that star formation activity of Onsala 1 could move from the west side of ultracompact H II region to the east side of two young stellar objects associated with the water masers. We also find that WMC1 and UC H II region could be gravitationally bound. Their relative velocity along the line of sight is  $\sim 3$  km s<sup>-1</sup>, and total mass is  $\sim 37M_{\odot}$ . Onsala 1 seems to harbor a binary star at different evolutionary stage.

**Key words:** Star: formation - ISM: H II region - ISM: individual (Onsala 1) - masers (water) - VLBI

## 1. Introduction

Star forming regions are often associated with water maser emissions, and the Very Long Baseline Interferometry (VLBI) monitoring observations of the water maser provide a unique tool to study the structure and kinematics of star forming region. Analyses of spatial positions, Doppler velocities, and proper motions of water masers have revealed the 3-D gas kinematics often in the vicinity of young stellar objects (YSOs) (e.g., Orion-KL: Genzel et al. 1981; Cepheus A: Torrelles et al. 2001; G192.16–3.84: Imai et al. 2006; G24.78+0.08: Moscadelli et al. 2007).

Onsala 1 star forming region (hereafter ON1) has an ultracompact (UC) H II region observed in radio continuum emissions at 8.4 GHz and 23.7 GHz (Zheng et al. 1985; Argon et al. 2000). Centimeter radio continuum luminosity of this UC H II region is  $10^{4.2}L_{\odot}$ , and indicates an exciting star of ZAMS type B0 (MacLeod et al. 1998). Kumar et al. (2004) reported the presence of multiple outflows from the UC H II region. One outflow traced by <sup>12</sup>CO  $J = 2-1$  line is elongated in the east-west direction with a velocity of 12 km s<sup>-1</sup> (respect to the systemic velocity of ON1  $V_{\text{LSR}} = 12$  km s<sup>-1</sup>), and other possible outflow traced by H<sup>13</sup>CO<sup>+</sup>  $J = 1-0$  line is elongated in the northeast-southwest direction with a velocity of 4.5 km s<sup>-1</sup> (Kumar et al. 2004). The H<sup>13</sup>CO<sup>+</sup> outflow is, however on the other hand, interpreted as a rotating disk by the observations in the NH<sub>3</sub> and same H<sup>13</sup>CO<sup>+</sup> lines (Zheng et al. 1985; Lim et al. 2002). These molecular

line observations suggest that there are several YSOs in or around the UC H II region of ON1.

Submillimeter continuum emission at 345 GHz (0.85 mm) using the Submillimeter Array (SMA) have resolved two components separated in the northeast–southwest direction (Su et al. 2004). The 345 GHz continuum emissions are elongated in the east side of the UC H II region. It is known that YSOs at the youngest stage often show spectral energy distribution with peak flux at submillimeter wavelength, originating from the dust envelopes (André et al. 1993). The strong submillimeter emissions from these two sources would, therefore, indicate that they are the youngest YSOs contained in ON1. Thus, YSOs at different evolutionary stages seem to be found in ON1.

VLBI observation of the water masers (Downes et al. 1979) shows that ON1 has two clusters of water masers separated by  $\sim 2''$  (3600 AU at our assumed distance of 1.8 kpc) in the northeast-southwest direction. These two clusters appear to have offsets from the core of the UC H II region traced by 23.7 GHz continuum emission (Zheng et al. 1985). This fact suggests that the water masers are associated with the newly YSOs which formed around the UC H II region. In order to confirm this, new multi-epoch VLBI observations to measure the proper motions of water masers are necessary.

The VLBI observation of Downes et al. (1979) detected water masers at  $V_{\text{LSR}} = 5-23$  km s<sup>-1</sup>. Kurtz & Hofner (2005) found that the water maser emission of ON1 has a larger velocity range ( $V_{\text{LSR}} = -53$  to 63 km s<sup>-1</sup>), and sug-

gested that these high velocity components would give an important information about other star formation signposts in ON1.

Here, we present the distribution and proper motions of 22.2 GHz water masers towards ON1. Section 2 describes the observations with the Japanese VLBI network (JVN, e.g., Doi et al. 2006; Imai et al. 2006) and data reduction. Section 3 shows the distribution and proper motion of the water masers. Section 4 discusses the driving sources of water masers and structure of ON1 through comparison with previous observations. The distance to ON1 is uncertain, however, a near kinematic distance of 1.8 kpc is favored by the most authors (e.g. MacLeod et al. 1998; Kumar et al. 2004). We therefore adopt the distance of 1.8 kpc to this source.

## 2. Observations

The VLBI observations of ON1 were made on March 24, and June 1, in 2005 and on January 8, in 2006 using five or six telescopes of the JVN composed of four 20-m telescopes of the VLBI Exploration of Radio Astrometry (VERA) of the National Astronomical Observatory of Japan (NAOJ), a 45-m telescope of the Nobeyama Radio Observatory (NRO), and a 34-m telescope of the National Institute of Information and Communications Technology (NiCT) at Kashima. ON1 and a calibrator source (ICRF J192559.6+210626) for clock parameter correction were observed for 10 hours in total per observing epoch. Left-hand circular polarization signals were recorded with the SONY DIR1000 recorder with a data rate of 128 Mbps and in two base band channels with a band width of 16 MHz each, covering a radial velocity span of  $215.7 \text{ km s}^{-1}$ . The data correlation was made with the Mitaka FX correlator (Chikada et al. 1991). The correlation outputs consisted of 1024 velocity channels, yielding frequency and velocity resolutions of 15.625 kHz and  $0.21 \text{ km s}^{-1}$ , respectively.

Data reduction was performed using the Astronomical Image Processing System (AIPS) of National Radio Astronomy Observatory (NRAO). Calibrations of the clock parameters, bandpass characteristics, visibility amplitudes, and phase visibility phases as well as velocity tracking were carried out in a standard manner. The clock parameters (clock offset and clock rate offset) were calibrated using the residual delay and delay rate for a calibrator source which was observed every hour. Bandpass calibration was made using auto correlation spectra of the continuum source. The amplitude calibration was made using the system noise temperatures; they were evaluated using the ‘‘R-Sky’’ method, by observing a reference black body at the beginning of each scan (typically every hour). Observed frequencies of maser lines were converted to the local-standard-of-rest (LSR) velocities using the rest frequency of 22.235080 GHz for  $\text{H}_2\text{O } 6_{16} - 5_{23}$  transition. For phase calibrations, the visibilities of all velocity channels were phase-referenced to the reference maser spot at a LSR velocity of  $16.5 \text{ km s}^{-1}$ , which is one of the brightest spots and it exhibits no sign of structure according to the closure phase deviation from zero. A typical size of

the synthesized beam was  $\sim 1$  milliarcseconds (mas) in the three observations (see Table 1).

We identified all emission components stronger than 7 times the rms noise level in the images for each spectral channel. Identification of a water maser feature, which represents a physical feature and consisting of a cluster of maser spots or velocity components was made by the procedure shown in several previous papers (e.g. Imai et al. 2000). We identified as the feature consisting of spots within a beam size of approximately 1 mas (1.8 AU). The feature position is defined as a brightness peak in the feature. Position uncertainties for the features were typically 0.05 mas. We detected 21, 18, and 23 maser features in the three epochs, respectively.

## 3. Results

### 3.1. Water Maser Spectrum

Figure 1 shows total power spectra of the ON1 water masers obtained with the Nobeyama 45-m and Mizusawa 20-m telescopes. There are low-velocity components ( $V_{\text{LSR}} \simeq 4\text{--}22 \text{ km s}^{-1}$ ) near the systemic velocity of ON1 observed in the  $\text{NH}_3$  line ( $V_{\text{LSR}} = 10\text{--}12 \text{ km s}^{-1}$ ; Zheng et al. 1985) and, in addition, high-velocity blue-shifted ( $V_{\text{LSR}} \simeq -60$  to  $-20 \text{ km s}^{-1}$ ), and red-shifted ( $V_{\text{LSR}} \simeq 50\text{--}60 \text{ km s}^{-1}$ ) components. The blue- and red-shifted components symmetrically appear around the systemic velocity. We have detected most of the velocity components seen in the previous observations (Downes et al. 1979; Kurtz & Hofner 2005).

The peak flux density of the low-velocity components is typically 100 Jy, and do not change from epoch to epoch. On the other hand, fluxes of the high-velocity components are time-variable. The blue-shifted components had 8 Jy in March 2005, and increased to more than 150 Jy in January 2006. These blue-shifted components were already found about 30 years ago by a singledish observation (Genzel & Downes 1977). However, they were too weak to be mapped by the VLBI in 1977 (Downes et al. 1979). The red-shifted components were strong (approximately 100–150 Jy) during our first and second VLBI observations (March–June 2005). However, they decreased to 30 Jy in January 2006. These redshifted components were not detected in 1977 and 1987, (Genzel & Downes 1977; Cesaroni et al. 1988), and detected for the first time in 1995 (Kurtz & Hofner 2005).

Statistics of water masers show that high-velocity components are generally highly variable, and are as weak as 0.1–10% of the low-velocity component (Genzel & Downes 1977). Similarly, the high-velocity component in ON1 is also highly variable. However, the high-velocity component is sometimes stronger than the low-velocity component. Its intensity is 10–200% of the low-velocity component.

### 3.2. Water Maser Distributions

Figure 2 shows distributions and the proper motion vectors of water masers in ON1 (for proper motions, see next subsection). 21 features detected at the first epoch are

plotted. The color index denotes the LSR velocity range from  $-41.8$  to  $58.4$  km s $^{-1}$ , where 21 features are located. The map origin is located at the position of the reference maser feature at  $V_{\text{LSR}} = 16.5$  km s $^{-1}$ , which is estimated to be  $\alpha(\text{J2000})=20^{\text{h}}10^{\text{m}}09^{\text{s}}201 \pm 0^{\text{s}}004$  and  $\delta(\text{J2000})=31^{\circ}31'36''.02 \pm 0''.08$  from fringe rate analysis. ON1 has two clusters of water maser features located at  $(X, Y) \simeq (0'', 0'')$  (hereafter WMC1 = water maser cluster 1) and at  $(X, Y) \simeq (-0''.9, -1''.4)$  (hereafter WMC2). The separation of WMC1 and WMC2 is  $1''.6$ , which corresponds to 2900 AU.

WMC1 is distributed within a region of  $\sim 320 \times 50$  mas ( $580 \times 90$  AU). The blue- ( $V_{\text{LSR}} = -41.8$  to  $-28.5$  km s $^{-1}$ ) and red-shifted ( $V_{\text{LSR}} = 52.4$ – $58.4$  km s $^{-1}$ ) maser features appeared in WMC1. Their separation is 195 mas, which corresponds to 350 AU. The blue- and red-shifted maser features are distributed within areas of  $9 \times 11$  mas ( $16 \times 20$  AU) and  $5 \times 14$  mas ( $9 \times 25$  AU), respectively, and were not detected outside these regions. The systemic velocity of WMC1 is  $V_{\text{LSR}} = 9.3 \pm 6.8$  km s $^{-1}$ , derived from three mean velocities of blue-shifted ( $V_{\text{LSR}} = -40.5 \pm 4.3$  km s $^{-1}$ ), red-shifted ( $V_{\text{LSR}} = 55.4 \pm 2.0$  km s $^{-1}$ ), and low-velocity ( $V_{\text{LSR}} = 13.1 \pm 3.2$  km s $^{-1}$ ) features detected in three epoch observations.

WMC2 is distributed within a region of  $\sim 160 \times 380$  mas ( $290 \times 680$  AU). Only the low-velocity features ( $V_{\text{LSR}} = 7.2$ – $14.8$  km s $^{-1}$ ) are detected in WMC2. The systemic velocity of WMC2 is derived to be  $V_{\text{LSR}} = 11.3 \pm 2.3$  km s $^{-1}$  from the mean velocity of low-velocity features detected in three epoch observations.

### 3.3. Proper Motions

Table 2 lists observed proper motions of 14 maser features in ON1. The maser features in different epochs were identified as the *same* feature, if their LSR velocities were equal to each other within  $0.42$  km s $^{-1}$  (2-channel) and if their positions were coincident within 2.5 mas at the first to second epoch and 7 mas at the second to third epoch. The spatial ranges of 2.5 and 7 mas correspond to the proper motion of  $100$  km s $^{-1}$  ( $12$  mas yr $^{-1}$ ). Based on these identification criteria, each maser feature was identified in at least two epochs. The proper motions have been calculated by performing a linear least-squares fit of the positional offsets to the elapsed time. Figure 3 shows observed time variations of right ascension and declination offsets (relative to feature “5”) of five features detected at all three epochs.

The proper motions of WMC1 exhibit a bipolar outflow structure in the east-west direction. The proper motions show high ( $69 \pm 11$  km s $^{-1}$ ) and low ( $\sim 10$  km s $^{-1}$ ) expansion velocities. The blue- and red-shifted features represent the high-velocity and collimated outflow. For the blueshifted features, the proper motion of the brightest feature at  $V_{\text{LSR}} = -40.5$  km s $^{-1}$  was obtained to be  $(\mu_x, \mu_y) = (7.9, -3.3)$  mas yr $^{-1}$ , which corresponds to  $(V_x, V_y) = (68, -28)$  km s $^{-1}$ . The mean proper motion of four redshifted features ( $V_{\text{LSR}} = 52.4$ – $58.4$  km s $^{-1}$ ) is  $(\mu_x, \mu_y) = (-3.0 \pm 0.7, 0.4 \pm 0.2)$  mas yr $^{-1}$ , which corresponds to  $(V_x, V_y) = (-25 \pm 6, 3 \pm 2)$  km s $^{-1}$ . These

proper motions appear to be associated with a common origin.

The simplest explanation for this fact is that the water masers in WMC1 are associated with a bipolar outflow which is ejected from a YSO located at the midpoint of the blue- and red-shifted features. The expansion velocity between the blue- and red-shifted features was estimated to be  $69 \pm 11$  km s $^{-1}$ , from the differences of their proper motions  $(\Delta V_x, \Delta V_y) = (93 \pm 6, 31 \pm 2)$  km s $^{-1}$  and LSR velocities  $\Delta V_{\text{LSR}} = 95 \pm 3$  km s $^{-1}$ . Inclination angle of the direction of expansion was determined to be  $44 \pm 3^\circ$ . The position angle and opening angle derived from the distributions of blue- and red-shifted features are  $92^\circ$  and  $10^\circ$ , respectively. The LSR velocities of three low-velocity features ( $V_{\text{LSR}} = 12.1, 15.0, 15.6$  km s $^{-1}$ ) in WMC1 show low expansion velocity ( $\sim 10$  km s $^{-1}$ ). Their LSR velocities are close to the LSR velocity of the quiescent molecular cloud observed in NH $_3$  line ( $V_{\text{LSR}} \sim 10$  km s $^{-1}$ ; Zheng et al. 1985). This may indicate an interaction between the outflow and the dense surrounding cloud (Genzel et al. 1981). Their proper motions are within  $\mu_x = 0.5$ – $1.5$ ,  $\mu_y = -0.5$  to  $-0.3$  mas yr $^{-1}$ , which correspond to  $V_x = 4$ – $13$ ,  $V_y = -4$  to  $-3$  km s $^{-1}$ .

The proper motions of WMC2 show  $\mu \sim 1$  mas yr $^{-1}$  ( $V \sim 10$  km s $^{-1}$ ). Although it is unknown what is associated with WMC2, the proper motions of WMC2 are not originated to WMC1. This indicates the presence of a driving source which is different from WMC1. Therefore, our proper motion measurements represent that there are at least two driving sources of water masers in ON1.

## 4. Discussion

### 4.1. Driving Sources of Water Masers

Figure 2(a) shows positions of the water masers relative to the 8.4 GHz continuum emission. The water masers are located at  $2''$  east from the peak of 8.4 GHz continuum emission with an absolute position accuracy of  $\approx 0''.3$  (Argon et al. 2000). The water masers are not coincident with the UC H II region and appear to be associated with the YSO formed on the east side of the UC H II region.

Submillimeter continuum emission traces dust emission around a YSO. The 345 GHz continuum emission observed with SMA has two components of north-eastern (SMA1) and south-western (SMA2) ones (Su et al. 2004). The water masers would be associated with SMA1 and SMA2. Water masers appear to have a position offset of approximately  $1''$  south-east from the both peak positions of 345 GHz continuum emission. This offset would be due to an insufficient angular resolution of the 345 GHz continuum observation of  $\sim 3''$  and insufficient absolute position accuracy.

A  $10.5$   $\mu\text{m}$  infrared source, which is not detected in the  $2.2$   $\mu\text{m}$  and  $3.75$   $\mu\text{m}$  emissions (Kumar et al. 2003), is situated near the center of the two WMCs and UC H II region. Because the  $10.5$   $\mu\text{m}$  emission is extended in a  $3'' \times 3''$  area, it is unclear whether this is associated with the present water maser features.

The total far-infrared luminosity of ON1 derived from

the IRAS data is  $10^{4.1}L_{\odot}$  and the luminosity of UC H II region observed in 1.3 to 20 cm radio continuum emission is  $10^{4.2}L_{\odot}$  (MacLeod et al. 1998). The agreement of the luminosities of far-infrared and radio continuum emissions indicates that ON1 has a single luminous star of spectral type of B0 ( $L \geq 10^4L_{\odot}$ ) which forms the UC H II region. The luminosities of YSOs in WMC1 and WMC2 seem to be lower ( $< 10^4L_{\odot}$ ) than that of the B0 star exciting the UC H II region.

We may thus conclude that the water masers WMC1 and WMC2 are associated with two YSOs on the eastern side of UC H II region. These two YSOs are still surrounded by dusty envelopes, emitting the 345 GHz submillimeter emission.

#### 4.2. Outflow and YSO in WMC1

The outflow of WMC1 is coincident with a jet-like outflow extended in the east-west direction by  $\sim 0.07$  pc, which was found by IRAM observations in the  $^{12}\text{CO } J = 2-1$  line (Kumar et al. 2004). The dynamical age of CO 2-1 outflow is estimated to be  $(5-7) \times 10^3$  yr using the LSR velocity difference from the systemic velocity of CO 2-1 ( $12 \text{ km s}^{-1}$ ) and the inclination angle of the outflow obtained by the present work ( $44 \pm 3^\circ$ ). The velocity spans in  $^{12}\text{CO } J = 1-0$  and 2-1 lines are  $35 \text{ km s}^{-1}$  and  $24 \text{ km s}^{-1}$ , respectively (Xu et al. 2006; Kumar et al. 2004). These values are smaller than the velocity span of water maser ( $\sim 100 \text{ km s}^{-1}$ ). This may be because the size of the high velocity outflow observed in the water masers ( $< 0''.2$ ) is too compact to be detected with the beam of the CO 1-0 ( $\sim 15''$ ) and CO 2-1 ( $\sim 2''$ ) lines. The dynamical age of the CO outflow of  $(5-7) \times 10^3$  yr suggests that the age of the YSO in WMC1 is about  $\sim 10^4$  yr.

Water maser features are most likely located in shock regions where the outflow from YSO hits ambient gases. We derive the momentum rate of the outflow in WMC1 using the method of Torrelles et al. (2003). The momentum rate is given by,

$$\dot{P}_f = 2\Omega_f R^2 \rho_f V_f^2, \quad (1)$$

where  $\Omega_f = 2\pi(1 - \cos(\theta_{\text{op}}/2))$  is the solid angle of the outflow,  $R$  the distance from the star,  $\rho_f$  the mass density in the outflow,  $V_f$  the expansion velocity of the outflow. Assuming a typical gas density necessary for water masering,  $n(\text{H}_2) = 10^8 \text{ cm}^{-3}$  (Elizur et al. 1992), the momentum rate of outflow can be estimated to be  $(1-2) \times 10^{-3} M_{\odot} \text{ yr}^{-1} \text{ km s}^{-1}$  for the observed expansion velocity ( $V_f = 69 \pm 11 \text{ km s}^{-1}$ ), the distance from the star ( $R = 175 \text{ AU}/\cos(44^\circ) = 245 \text{ AU}$ ), and the opening angle ( $\theta_{\text{op}} = 10^\circ$ ). In addition, using this momentum rate and dynamical age derived from the CO 2-1 outflow, we can estimate the momentum of the outflow in WMC1 to be  $5-14 M_{\odot} \text{ km s}^{-1}$ . This value is 10-30% of the momentum of the largest outflow in ON1 with a size of 0.94 pc found in  $^{12}\text{CO } J = 1-0$  line (Xu et al. 2006). Therefore, the outflow in WMC1 would not mainly contribute to the formation of the CO 1-0 outflow.

#### 4.3. Star Formation Activity of ON1

Dense molecular gas, which is traced in CS  $J = 5-4$  line (Shirley et al. 2003) and dust emission at  $350 \mu\text{m}$  (Mueller et al. 2002), extend to the east and north side of the UC H II region. The different locations of the UC H II region, submillimeter continuum emissions, water masers, and dense molecular cloud suggest that the star formation activity of ON1 moves from west to east. In Table 3, we summarize the possible properties of B0 star exciting the UC H II region as well as the YSO associated with WMC1 and WMC2. The mass of star in UC H II region is  $\sim 15M_{\odot}$ , which indicated by the spectral type of approximately B0 (MacLeod et al. 1998). The mass of YSO in WMC1 would be  $\sim 2-15 M_{\odot}$ , because the momentum rate of the outflow in WMC1 corresponds to a typical value of intermediate-mass YSO (Shepherd 2005). The difference between WMC1 and WMC2 is only the expansion velocity of water masers. This velocity difference may reflect the difference of outflow energy between WMC1 and WMC2. This indicates lower power, implying a lower mass of the forming YSO in WMC2 than in WMC1.

Finally, we propose that the B0 star is the possible driving source of the CO 1-0 outflow. The dynamical age of CO 1-0 outflow is estimated to be  $7.3 \times 10^4$  yr at our assumed distance (Xu et al. 2006). Thus, we think the age of the B0 star is  $\sim 10^5$  yr.

#### 4.4. A Binary System Formed by WMC1 and UC H II Region?

The LSR velocities of WMC1 and UC H II region is estimated to be  $V_{\text{LSR}} = 9.3 \pm 6.8$ , and  $12.3 \pm 3.5 \text{ km s}^{-1}$ , from the systemic velocities of water masers and OH masers (Fish et al. 2005), respectively. If WMC1 and UC H II region were separated at a relative velocity of  $3 \text{ km s}^{-1}$  during the formation timescale of B0 star exciting the UC H II region of  $\sim 10^5$  yr, WMC1 and UC H II region should already be separated by  $\sim 60000 \text{ AU}$  (0.30 pc). However, their separation on the sky is  $3600 \text{ AU}$  (0.017 pc). Therefore, we may consider that WMC1 and UC H II region are gravitationally bound. Assuming that WMC1 and UC H II region are gravitationally bound, that total mass ( $M_t$ ) can be estimated by,

$$M_t \sim \frac{Rv^2}{G} \quad (2)$$

$$\sim 4.1 \times \left( \frac{R}{3600 \text{ AU}} \right) \left( \frac{v}{1 \text{ km s}^{-1}} \right)^2 M_{\odot} \quad (3)$$

where,  $R$  is a separation of the WMC1 and UC H II region and  $v$  is the relative velocity. This total mass is minimum value, because the separation along the line of sight and the relative velocity of the sky are still unknown. The total mass is derived  $M_t \sim 37M_{\odot}$  from the separation of  $3600 \text{ AU}$  and the relative velocity of  $v = 3 \text{ km s}^{-1}$ . The masses of 345 GHz dust emission core associated with the WMC1 and UC H II region are estimated to be  $6 M_{\odot}$ , and  $6 M_{\odot}$ , respectively (Su et al. 2006). Therefore, the total mass YSO and B0 star, and accompanying dust-emission cores is  $\sim 29-42 M_{\odot}$ . This value is consistent

with the total mass estimated on the basis of assumption of a gravitationally bound system. Therefore, we propose that the YSO in WMC1 and B0 star exciting the UC H II region form a binary star. The LSR velocity of WMC2 ( $V_{\text{LSR}} = 11.3 \pm 2.3 \text{ km s}^{-1}$ ) indicates that the YSO in WMC2 is a third object of this bound system.

In Figure 4, we illustrate a possible structure of ON1, as inferred from the present consideration based on Figure 2(a). A rotating disk is found in  $\text{NH}_3$  ( $J, K$ ) = (1, 1), and  $\text{H}^{13}\text{CO}^+$   $J = 1-0$  lines with the VLA and the BIMA array (Zheng et al. 1985; Lim et al. 2002). The orbit in Figure 4 is assumed to be at a position angle of  $40^\circ$  which is seen in the velocity gradient in  $\text{H}^{13}\text{CO}^+$  line (Lim et al. 2002).

## 5. Conclusions

The following conclusions are drawn from this study:

1. We carried out three epoch observations of the ON1 water masers with the JVN, and successfully measured the proper motions of ON1 water masers for the first time.
2. ON1 has two major water maser clusters (WMC1 and WMC2) which are separated by 2900 AU. Both the WMCs are located at 3600 AU from the UC H II region seen at 8.4 GHz continuum emission.
3. Proper motion measurement reveals that WMC1 is associated with a bipolar outflow elongated in the east-west direction with high expansion velocity of  $69 \pm 11 \text{ km s}^{-1}$ . This outflow is coincident with a jet-like outflow found in CO 2-1 line.
4. The WMC1 and WMC2 are associated with two 345 GHz continuum sources on the east side of the UC H II region. These two YSOs are still surrounded by dusty envelopes.
5. The star formation activity of ON1 appears to move from west side of the UC H II region to east side of two WMCs and dense molecular cloud observed in CS lines.
6. We suggests that the WMC1 and UC H II region in ON1 form a binary system. The relative velocity and total mass of WMC1 and UC H II region are estimated to be  $\Delta V_{\text{LSR}} \sim 3 \text{ km s}^{-1}$  and  $M_t \sim 37 M_\odot$ , respectively.

The authors wish to thank to all staff members and students of VERA team for observing assistance and support. We hope VERA observe one thousand of water maser sources to perform the astrometry of galactic star forming regions and investigate the structure and dynamics of the Milky Way Galaxy. We thank an anonymous referee for very useful comments. T.O. and H.I. were supported by a Grant-in-Aid for Scientific Research from Japan Society for Promotion Science (17340055).

## References

André, P., Ward-Thompson, D., & Barsony, M. 1993, *ApJ*, 406, 122

- Argon, A. L., Reid, M. J., & Menten, K. M. 2000, *ApJS*, 129, 159
- Cesaroni, R., Palagi, F., Felli, M., Catarzi, M., Comoretto, G., di Francos, Giovanardi, C., & Palla, F. 1988, *A&AS*, 76, 445
- Chikada, Y., et al. 1991, in *Frontiers of VLBI*, ed. H. Hirabayashi, M. Inoue, & H. Kobayashi (Tokyo: Universal Academy Press), 79
- Doi, A., et al. 2006, *PASJ*, 58, 777
- Downes, D., Genzel, R., Moran, J. M., Johnston, K. J., Matveenko, L. I., Kogan, L. R., Kostenko, V. I., & Ronnang, B. 1979, *A&A*, 79, 233
- Elitzur, M., Hollenbach, D. J., & McKee, C. F. 1992, *ApJ*, 394, 221
- Fish, V. L., Reid, M. J., Argon, A. L., & Zheng, X. W. 2005, *ApJS*, 160, 220
- Genzel, R., & Downes, D. 1977, *A&AS*, 30, 145
- Genzel, R., Reid, M. J., Moran, J. M., & Downes, D. 1981, *ApJ*, 244, 884
- Imai, H., Kameya, O., Sasao, T., Miyoshi, M., Deguchi, S., Horiuchi, S., & Asaki, Y. 2000, *ApJ*, 538, 751
- Imai, H., Omodaka, T., Hirota, T., Umamoto, T., Sorai, K., & Kondo, T. 2006, *PASJ*, 58, 883
- Kumar, M. S. N., Bachiller, R., & Davis, C. J. 2002, *ApJ*, 576, 313
- Kumar, M. S. N., Davis, C. J., & Bachiller, R. 2003, *Ap&SS*, 287, 191
- Kumar, M. S. N., Tafalla M., & Bachiller, R. 2004, *A&A*, 426, 195
- Kurtz, S., & Hofner, P. 2005, *AJ*, 130, 711
- Lim, J., Choi, M., & Ho, P. T. P. 2002, *ASPC*, 267, 385
- MacLeod, G. C., Scalise, E. J., Saedt, S., Galt, J. A., & Gaylard, M. J. 1998, *AJ*, 116, 1897
- Moscadelli, L., Goddi, C., Cesaroni, R., Beltrán, M. T., & Furuya, R. S. 2007, *A&A*, 472, 867
- Mueller, K. E., Shirley, Y. L., Evans, N. J., & Jacobson, H R. 2002, *ApJS*, 143, 469
- Shepherd, D. 2005, in *IAU Symp. 227*, ed. R. Cesaroni, M. Felli, E. Churchwell, & M. Walmsley (Cambridge: Cambridge Univ. Press), 237
- Shirley, Y. L., Evans, N. J. II, Young, K. E., Knez, C., & Jaffe, D. T. 2003, *ApJS*, 149, 375
- Su, Y. N., et al. 2004, *ApJ*, 616, 39
- Su, Y. N., Liu, H. R., & Lim, J. 2006, in the proceedings of the East Asian Young Astronomers Meeting 2006, Y. Urata, D. Kinoshita, T. Sekiguchi, A. Yonehara eds. (National Astronomical Observatory of Japan: Mitaka), p17
- Torrelles, J. M., et al. 2001, *ApJ*, 560, 853
- Torrelles, J. M., et al. 2003, *ApJ*, 598, L115
- Xu, Y. et al. 2006, *AJ*, 132, 20
- Zheng, X. W., Ho, P. T. P., Reid, M. J., & Schneps, M. H. 1985, *ApJ*, 293, 522

**Table 1.** Status of the telescopes, data reduction, and resulting performances in the individual epochs of the JVN observations.

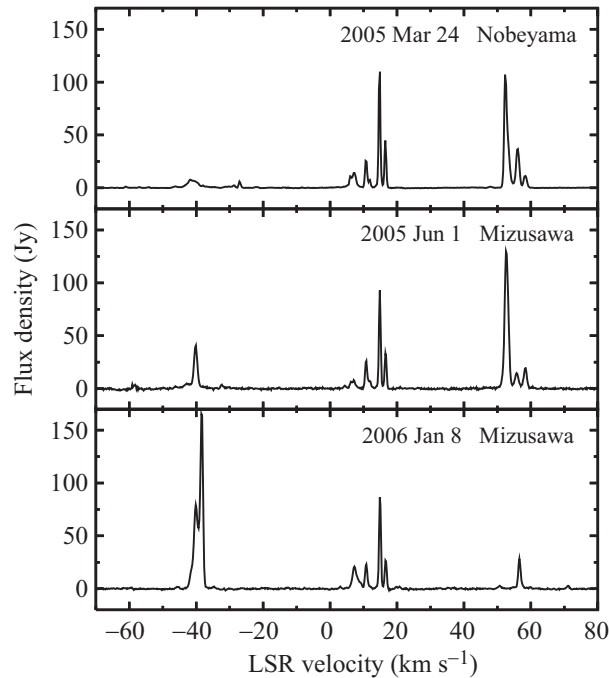
Epoch	Date	Duration (hr)	Used telescopes*	Reference velocity <sup>†</sup> (km s <sup>-1</sup> )	1- $\sigma$ level noise (Jy beam <sup>-1</sup> )	Synthesized beam <sup>‡</sup> (mas)	Number of detected features
1 ...	2005 Mar 24	10	MZ, IR, OG, IS, KS <sup>§</sup> , NB	16.5	0.045	$1.9 \times 0.7, -38^\circ$	21
2 ...	2005 Jun 1	10	MZ, OG, IS, KS, NB	16.5	0.032	$3.4 \times 1.3, -86^\circ$	18
3 ...	2006 Jan 8	10	MZ, IR, OG, IS, KS	16.5	0.039	$1.7 \times 0.9, -51^\circ$	23

\* Telescopes that were effectively operated and whose recorded data were valid: MZ: the VERA 20-m telescope at Mizusawa, IR: the VERA 20-m telescope at Iriki, OG: the VERA 20-m telescope at Ogasawara Is, IS: the VERA 20-m telescope at Ishigakijima Is, KS: the NiCT 34-m telescope at Kashima, NB: the NRO 45-m telescope at Nobeyama.

<sup>†</sup> Local-standard-of-rest velocity of the spectral channel used for the phase reference in data reduction.

<sup>‡</sup> The synthesized beam made in natural weight; major and minor axis lengths and position angle.

<sup>§</sup> Ceasing operation for 8 hours due to strong winds.

**Fig. 1.** The spectra of total flux of ON1 water masers, obtained in the three epochs with the Nobeyama 45-m and the Mizusawa 20-m telescopes. The velocity resolution is equal to the channel width of 0.21 km s<sup>-1</sup>.

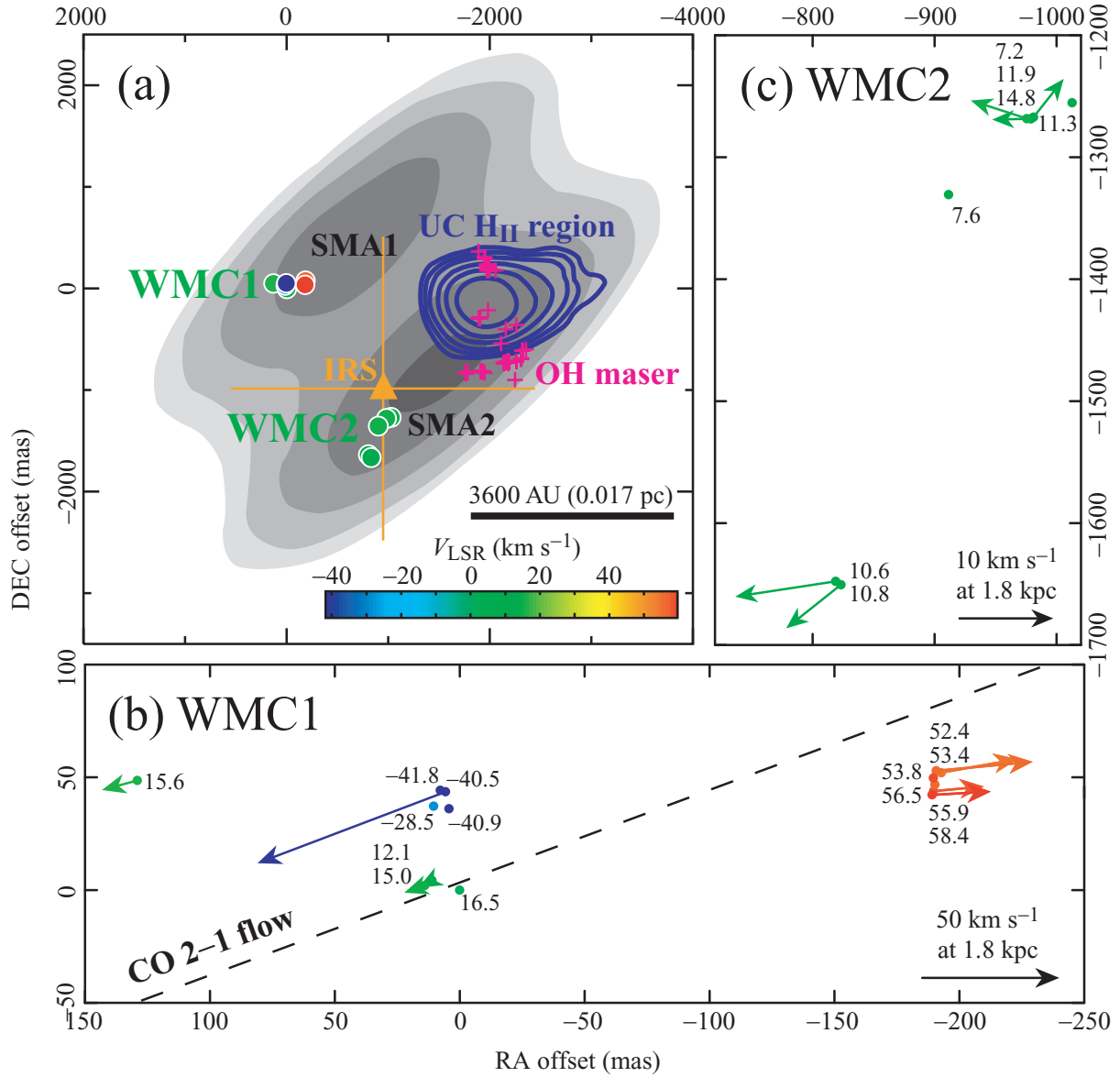


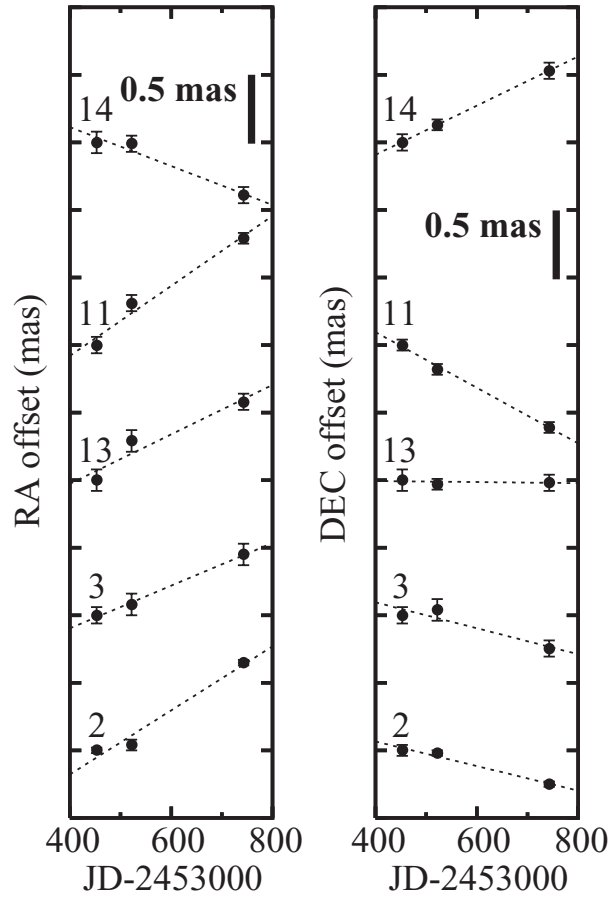
**Fig. 2.** (a): Observed water maser distributions (colored filled circle) superimposed on an 8.4 GHz radio continuum map (thick contour) of the UC H II region (Argon et al. 2000). The grey-scale map shows the 345 GHz radio continuum showing dust emission (Su et al. 2004), where the lowest grey contour indicates a half of the peak brightness. Crosses show OH maser distribution (Fish et al. 2005) and triangle indicates the  $10\mu\text{m}$  infrared source (Kumar et al. 2003). The map origin with RA and DEC offsets = (0, 0) is at  $\alpha(J2000)=20^{\text{h}}10^{\text{m}}09^{\text{s}}201 \pm 0^{\text{s}}004$  and  $\delta(J2000)=31^{\circ}31'36''02 \pm 0''08$ . 1000 mas corresponds to 1800 AU at a distance of 1.8 kpc. (b), (c): Close-up to the two water maser clusters (WMC1 and WMC2) with proper motion vectors. The colored arrows and number added for each feature denote LSR velocity. The arrows at the bottom-right corner in (b) and (c) indicate a proper motion of 5.9 mas yr<sup>-1</sup> and 1.2 mas yr<sup>-1</sup> (50 km s<sup>-1</sup> and 10 km s<sup>-1</sup>), respectively. The dashed line in (b) indicates the axis of bipolar outflow observed in <sup>12</sup>CO  $J = 2-1$  line (Kumar et al. 2004)

**Table 2.** Parameters of the water maser features identified by proper motion toward ON1.

ID*	Offset <sup>†</sup> (mas)				LSR velocity (km s <sup>-1</sup> )	Proper motion <sup>†</sup> (mas yr <sup>-1</sup> )				Peak intensity at three epochs (Jy beam <sup>-1</sup> )		
	<i>X</i>	$\sigma X$	<i>Y</i>	$\sigma Y$		$V_{\text{LSR}}$	$\mu_x$	$\sigma\mu_x$	$\mu_y$	$\sigma\mu_y$	Epoch 1	Epoch 2
1	129.04	0.05	48.58	0.05	15.69	1.49	...	-0.44	...	0.40	...	0.65
2	13.99	0.01	1.98	0.02	15.06	0.86	0.15	-0.33	0.05	13.70	15.00	21.50
3	11.04	0.03	4.29	0.03	12.11	0.57	0.03	-0.34	0.13	1.03	0.81	0.56
4	5.69	0.06	43.55	0.08	-40.54	7.93	...	-3.33	...	0.53	6.82	...
5	0.00	0.06	0.00	0.04	16.53	0.00	...	0.00	...	6.55	6.75	5.28
6	-189.05	0.02	42.17	0.02	58.45	-2.48	...	0.15	...	3.09	5.50	...
7	-189.71	0.02	43.91	0.02	55.93	-2.11	...	0.21	...	7.53	3.69	...
8	-190.73	0.01	52.90	0.01	53.40	-4.07	...	0.42	...	10.60	17.90	...
9	-192.73	0.01	52.05	0.01	52.56	-3.22	...	0.63	...	28.00	26.00	...
10	-818.83	0.13	-1647.78	0.07	10.64	1.73	...	-0.26	...	...	1.63	1.90
11	-823.19	0.03	-1650.52	0.02	10.85	0.94	0.16	-0.75	0.04	2.96	2.67	3.69
12	-975.58	0.07	-1268.37	0.06	14.85	0.96	...	0.31	...	1.31	...	0.66
13	-978.89	0.04	-1268.50	0.04	11.90	0.66	0.20	-0.01	0.03	0.89	1.16	0.71
14	-981.02	0.04	-1267.26	0.03	7.27	-0.52	0.11	0.66	0.00	2.23	1.30	0.86

\* Feature ID number.

† Relative value with respect to the position-reference maser feature: ID 5.

**Fig. 3.** Observed relative proper motions of water maser features in ON1. The proper motions of only the maser features detected at all three epochs are presented. A number added for each sub-panel shows the assigned one listed in Table 2. The dash line indicates a least-squares-fitted line assuming a constant velocity motion.



**Table 3.** Properties of B0 star in UC H II region and YSOs in WMC1 and WMC2.

No	Name	Emission	Maser	Velocity span* (km s <sup>-1</sup> )	Luminosity (L <sub>⊙</sub> )	Age <sup>†</sup> (yr)	Mass <sup>‡</sup> (M <sub>⊙</sub> )
1 ...	B0 star	Ionized gas <sup>§</sup> + Dust <sup>  </sup>	OH <sup>#</sup>	~ 15 <sup>#</sup>	10 <sup>4.2**</sup>	~ 10 <sup>5</sup>	~ 15
2 ...	WMC1 YSO	Dust <sup>§</sup>	Water	~ 100	< 10 <sup>4††</sup>	~ 10 <sup>4</sup>	~ 2–15 M <sub>⊙</sub>
3 ...	WMC2 YSO	Dust <sup>  </sup>	Water	~ 10	< 10 <sup>4††</sup>	...	≤ 2–15 M <sub>⊙</sub>

\* LSR velocity span of masers.

† Estimated ages of B0 star and WMC1 YSO (see subsection 4.2 and 4.3).

‡ Estimated masses (see subsection 4.3).

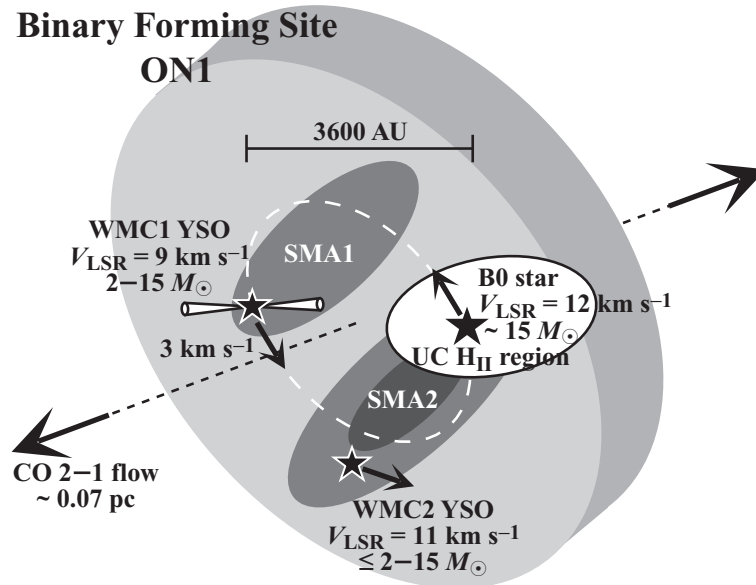
§ Traced by 8.4 GHz continuum emission (Argon et al. 2000).

|| Traced by 345 GHz continuum emission (Su et al. 2004).

# Results obtained in OH maser observation (Fish et al. 2005).

\*\* Luminosity obtained in 1.3 to 20 cm radio continuum emissions (MacLeod et al. 1998).

†† Luminosity estimated from the far-infrared and radio continuum emissions (see subsection 4.1).

**Fig. 4.** Schematic representation of the structure of ON1.